land.

[1]See, for example, J. D. Eshelby, in *Solid State Physics*, edited by F. Seitz and D. Turnbull (Academic, New York, 1956), Vol. 3, p. 105.

[2]P. A. Sturrock, in *Plasma Hydromagnetics*, edited by D. Bershader (Stanford U. P., Stanford, California, 1962).

[3]V. B. Fiks, Fiz. Tverd. Tela 3, 994 (1961) [Sov. Phys. Solid State 3, 724 (1961)].

[4]J. Wilks, *The Properties of Liquid and Solid Helium* (Clarendon, Oxford, England, 1967).

[5]M. Gerl, Z. Naturforsch. 26a, 1 (1971).

[6]H. B. Huntington, J. Phys. Chem. Solids 29, 1641 (1968).

[7]See, for example, R. E. Howard and A. B. Lidiard, Rept. Progr. Phys. 27, 161 (1964); N. L. Peterson, in *Solid State Physics*, edited by F. Seitz, D. Turnbull, and H. Ehrenreich (Academic, New York, 1968), Vol. 22.

[8]G. Schottky, Phys. Status Solidi 8, 357 (1965).

[9]See, for example, A. R. Allnatt, Z. Naturforsch. 26a, 10 (1971), and references cited therein.

[10]C. P. Flynn and A. M. Stoneham, Phys. Rev. B 1, 3966 (1970); J. A. Sussman, J. Phys. Chem. Solids 28, 1643 (1967).

[11]M. D. Feit, Phys. Rev. B 3, 1223 (1971).

[12]L. Brillouin, *Tensors in Mechanics and Elasticity* (Academic, New York, 1964).

[13]We are neglecting the contribution $-\partial V_{\text{anh}}/\partial \tilde{u}_n$ evaluated at $\langle \tilde{u}_1 \rangle$, $\langle \tilde{u}_2 \rangle, \ldots, \langle \tilde{u}_n \rangle$, since this term is clearly of order $\langle u \rangle \langle u \rangle$. In our development we do, however, retain terms of order $\langle uu \rangle$; these terms are of order $\langle u \rangle$, as our result (7) implies.

[14]R. J. Elliot, in *Phonons in Perfect Lattices and in Lattices with Point Imperfections*, edited by R. W. H. Stevenson (Oliver and Boyd, Edinburgh, 1966).

[15]A. A. Maradudin, Rept. Progr. Phys. 28, 331 (1965).

[16]R. S. Sorbello, Ph.D. thesis (Stanford University, 1970) (unpublished).

[17]Result (11) for scattering states is identical in form to that obtained for eigenstates in Ref. 15.

[18]A. A. Maradudin, in *Phonons and Phonon Interactions*, edited by T. A. Bak (Benjamin, New York, 1964).

[19]Use the model of Sec. III and write the force of local thermal expansion as the product of K_1 and the local thermal expansion $a\alpha T$, where α is the thermal expansion coefficient and T is some effective temperature. Express α as $K_2 k/K_1^2 a$, where k is Boltzmann's constant [see, e.g., C. Kittel, *Introduction to Solid State Physics*, 4th ed. (Wiley, New York, 1971), p. 222]. Then notice that the force of local thermal expansion is identical to the phonon-radiation force, Eq. (12), if the identification $kT = 2\langle V \rangle$ is made.

[20]Our estimate for the current arising from the Schottky mechanism may be in some error because we have not considered how the activation energy is distributed among the atoms during the diffusion jump. For an estimation of this effect based on the Wirtz–Brinkman model see Ref. 6 and H. B. Huntington, M. D. Feit, and D. Lortz [Crystal Lattice Defects 1, 193 (1970)]. The modifications introduced by the Wirtz–Brinkman model, however, are expected to affect the currents from the Schottky mechanism and from the phonon-radiation force in substantially the same way. Our estimate of the relative importance of the two currents would then still hold.

[21]An estimate can be made of the effect of the phonon-radiation force on mass-isotope impurity migration in a temperature gradient. To do this, we use expression (15), and take a perturbed Bose distribution for phonons in the relaxation-time approximation. Assuming a Debye model for the lattice, it then can be shown (Ref. 16) that to first order in the relative mass difference ϵ, the phonon-radiation force gives rise to a heat of transport estimated by $\epsilon \omega_D \tau \gamma k T$, where ω_D is the Debye frequency and τ is the phonon relaxation time.

PHYSICAL REVIEW B VOLUME 6, NUMBER 12 15 DECEMBER 1972

Symmetry of Quadratic-Mode Absorption and Emission Band Shapes of Impurities in Solids

C. Stuart Kelley

Chemical Laboratory, Edgewood Arsenal, Maryland 21010

(Received 13 July 1972)

Absorption and emission spectra are calculated for impurities that interact with the lattice by a quadratic mode. With different vibrational energies for the ground and excited states, the spectra are near mirror images at $T=0$, and virtually identical well above $T=0$. The emission line spacing differs from that of the absorption lines, and the high-temperature emission spectrum is identical with the absorption spectrum at an effective temperature that involves the ratio of the excited-state and ground-state vibrational energies. This ratio can be found from the peak intensities of the high-temperature absorption and emission spectra.

The absorption and emission spectra of an impurity in a solid contain lines due to purely electronic transitions (zero-phonon transitions, or those producing no change in the vibrational state of the lattice) and electronic transitions that are accompanied by changes in the vibrational state of the lattice (phonon-assisted transitions).[1-3] At very low temperatures, the electronic transitions are accompanied only by phonon emission, and the emission spectrum is very near the mirror image of the absorption spectrum, as rotated about the zero-phonon line. Using this aspect of the spectra, zero-phonon lines can be identified from phonon-assisted bands.[4,5] The present arti-

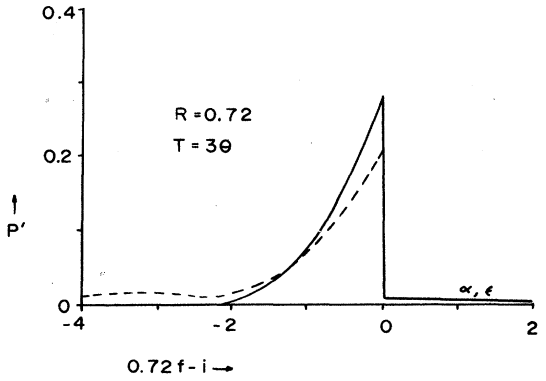

FIG. 1. Absorption (solid line) and emission (dotted line) line shapes for $R = 0.72$ at $T = 3\theta$. The half-width of the emission band is greater than that of the absorption band, a consequence of $R < 1$.

cle concerns the extent to which this mirror symmetry of the spectra occurs.

The impurity is treated quantum mechanically as a single-mode system in which the ground- and excited-states are harmonic oscillators having different vibrational frequencies. The minimum of the excited-state potential-energy curve in configuration coordinate space is displaced from that of the ground state by the energy E_0 and the configuration coordinate q_0. Matrix elements for transitions between vibrational levels of the ground and excited states have been derived for cases in which q_0 is either finite or zero.[6] The model considered here is for small q_0, a situation applicable to impurity centers located at sites of inversion symmetry. Within the harmonic and adiabatic approximations, matrix elements[7] for optical transitions are combined with appropriate thermal population factors to give the normalized absorption spectrum

$$P'_\alpha(E,T) = \frac{P_\alpha(E,T)}{C\langle\phi|e\vec{r}|\phi'\rangle^2} = \frac{2\sqrt{R}}{1+R}(1-e^{-\theta/T}) \times \sum_{i,f=0}^{\infty} \frac{f!}{i!}\left[L_{(i+f)/2}^{(i-f)/2}\left(\frac{2\sqrt{R}}{1+R}\right)\right]^2 e^{-i\theta/T} \times \delta[E - E_{zp} - (Rf - i)\hbar\omega] \quad . \quad (1)$$

The probability $P_\alpha(E, T)$ of absorption at energy E and temperature T is given in terms of the constant C and the matrix element $\langle\phi|e\vec{r}|\phi'\rangle$ of the electric dipole transition. The ratio of the excited-state vibrational frequency ω' to that of the ground state ω is R; f and i are the quantum numbers of the excited and ground states, and $\theta = \hbar\omega/k$. The functions $L_\nu^\mu(x)$ are associated Legendre polynomials. δ functions indicate the locations of the absorptions, and the factors preceding them are the absorption intensities. The energy $E_{zp} = E_0 + \frac{1}{2}(R-1)\hbar\omega$ locates the zero-phonon transition. The selection rule is that $i+f$ must be even.

Because the wave functions are real, the matrix elements for emission are the same as those for absorption. Using the thermal population factor appropriate to the excited state, the probability of emission is

$$P'_\epsilon(E,T) = \frac{P_\epsilon(E,T)}{C\langle\phi|e\vec{r}|\phi'\rangle^2} = \frac{2\sqrt{R}}{1+R}(1-e^{-R\theta/T}) \times \sum_{i,f=0}^{\infty} \frac{f!}{i!}\left[L_{(i+f)/2}^{(i-f)/2}\left(\frac{2\sqrt{R}}{1+R}\right)\right]^2 e^{-fR\theta/T} \times \delta[E - E_{zp} - (Rf - i)\hbar\omega] \quad . \quad (2)$$

It will be seen from Eqs. (1) and (2) that the absorption and emission spectra are identical except for the differences in the thermal population factors.

At $T = 0$,

$$P'_\alpha(E,0) = \frac{2\sqrt{R}}{(1+R)}\sum_{m=0}^{\infty}\frac{(2m)!}{4^m(m!)^2}\left(\frac{1-R}{1+R}\right)^{2m} \times \delta[E - E_{zp} - 2mR\hbar\omega]$$

and

$$P'_\epsilon(E,0) = \frac{2\sqrt{R}}{(1+R)}\sum_{n=0}^{\infty}\frac{(2n)!}{4^n(n!)^2}\left(\frac{1-R}{1+R}\right)^{2n} \times \delta[E - E_{zp} + 2n\hbar\omega] \quad ,$$

where both $m = f/2$ and $n = i/2$ can assume all positive integer values. The absorption spectrum at $T = 0$ consists of a series of spikes whose intensities decrease with increasing energy and which have a low-energy cutoff at the zero-phonon line. Conversely, the emission spectrum has a high-energy cutoff at E_{zp} and a low-energy tail. The intensities of corresponding transitions (e.g., $i = 0 \rightarrow f = 2$ in absorption, and $f = 0 \rightarrow i = 2$ in emission) are equal, a consequence of $T = 0$. Only the zero-phonon line is common to both spectra. The mirror symmetry of the spectra is marred only by the line spacings; the spacing of absorption lines is R times that of the emission line spacing. Thus with $R = 1 + \Delta$, the $T = 0$ absorption spectrum is broader than the emission spectrum for $\Delta > 0$, narrower for $\Delta < 0$.

This near mirror symmetry is altered when $T > 0$, as illustrated by the figures. These were obtained from calculation of Eqs. (1) and (2) by computer. The spikes of each spectrum cluster by values of $2\gamma = f - i$, where γ is any positive integer. Accordingly, the envelopes of these clusters were drawn and summed to give the total absorption and emission band shapes. While this procedure of using the envelopes instead of the individual spikes may eliminate some of the fine

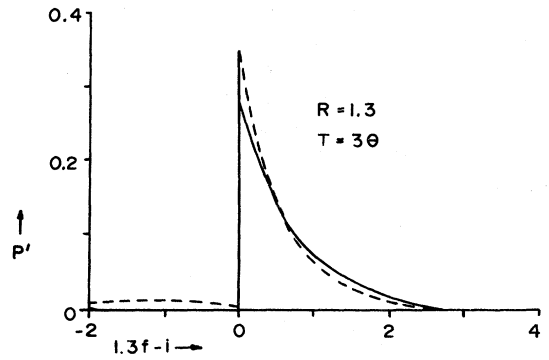

FIG. 2. Absorption (solid line) and emission (dotted line) line shapes for $R=1.3$ at $T=3\theta$. Because $R>1$, the peak of the emission band is more intense than that of the absorption band.

structure, it is equivalent to providing each spike with a finite half-width, that would be introduced in experimental data by crystal strains, or other deviations from the approximations used in the derivation of Eq. 1. The dominant transitions are for $\gamma=0$. There is no mirror symmetry, and the spectra are nearly identical. The only difference in the spectra is that the emission spectrum is the absorption spectrum at an effective temperature $T_{eff}=T/R$.

The absorption and emission envelopes peak at E_{zp}, and the strongest contribution near this energy is from transitions between $i=0$ and $f=0$. Approximating the peak intensities of the spectra by the intensities of the zero-phonon transitions and considering high temperatures $T \gtrsim \theta$, one then obtains from Eqs. (1) and (2), $P_\epsilon/P_\alpha \simeq R$. The spectra in Figs. 1–3 give $P_\epsilon/P_\alpha = 0.74$, 1.24, and 0.73, compared to the R values of 0.72, 1.3, and 0.72, respectively.

The intensity of a particular transition depends on both the overlap of the ground- and excited-state wave functions (i.e., a small γ produces a large overlap) and the thermal population factor (for absorption, a small i produces a large line intensity). Because the most intense lines are those for which $\gamma=0$, the transition intensity is more highly sensitive to γ than to the thermal population factor. This implies that the over-all band shape is not very temperature dependent, as may be seen from the figures for high temperatures. At low temperatures, the primary effect is the broadening of the spectra.

With $f=i+2\gamma$ and $R=1+\Delta$, the most intense ($\gamma=0$) absorption and emission spikes occur at $E=E_{zp}+i\Delta\hbar\omega$. Thus the dominant spikes of the spectra for $R<1$ and $R>1$ are rotated about the zero-phonon line from each other, and lie below and above the zero-phonon line, respectively. Other peaks are also rotated by $i\Delta\hbar\omega$ due to a sign change in Δ, but they are additionally shifted by $2\gamma(1+\Delta)\hbar\omega$. Nevertheless, the intense portion of the absorption (or emission) spectrum is rotated about the zero-phonon line if Δ changes sign. For $\Delta=0$ the absorption and emission spectra consist of a single line at E_0, because the only allowed transitions are for $\gamma=0$.

From the absorption (emission) spectrum near $T=0$, the separation $\Delta E_\alpha=\hbar\omega'=R\hbar\omega$ ($\Delta E_\epsilon=\hbar\omega$) of the zero- and first-phonon-assisted transitions and the ratio $P_{\alpha 0}/P_{\alpha 1}=(1-R)^2/2(1+R)^2$ ($=P_{\epsilon 0}/P_{\epsilon 1}$) of their intensities can be used to determine ω'

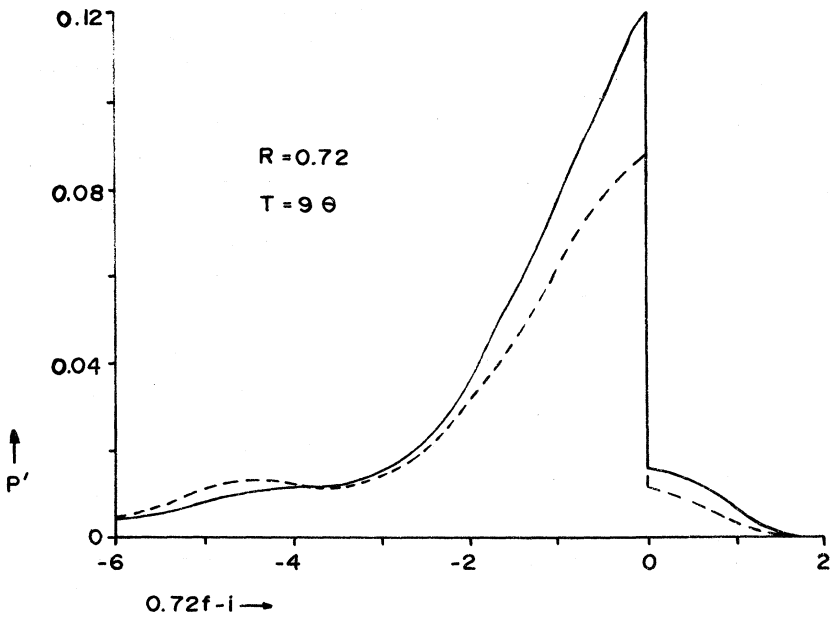

FIG. 3. High-temperature absorption (solid line) and emission (dotted line) line shapes for $R=0.72$ at $T=9\theta$. The ratio of the peak intensities of the emission and absorption bands is R.

$= \Delta E_\alpha/\hbar$, $\omega = \Delta E_\epsilon/\hbar$, and

$$R = \frac{1-(2P_{\alpha 0}/P_{\alpha 1})^{1/2}}{1+(2P_{\alpha 0}/P_{\alpha 1})^{1/2}} .$$

Additionally, R can be approximated as the ratio $P_{\epsilon\,max}/P_{\alpha\,max} = R$ of the peak intensities of the high-temperature emission and absorption spectra.

[1]C. S. Kelley and F. E. Williams, Phys. Rev. B 2, 3 (1970).

[2]F. E. Williams, J. Chem. Phys. 19, 457 (1951).

[3]J. T. Vallin, G. A. Slack, S. Roberts, and A. E. Hughes, Phys. Rev. B 2, 4313 (1970).

[4]F. S. Ham and G. A. Slack, Phys. Rev. B 4, 777 (1971).

[5]G. A. Slack and B. M. O'Meara, Phys. Rev. 163, 335 (1967).

[6]T. H. Keil, Phys. Rev. 140, A601 (1965).

[7]C. S. Kelley, Technical Report No. 4426, Edgewood Arsenal, Md., 1970 (unpublished).

PHYSICAL REVIEW B VOLUME 6, NUMBER 12 15 DECEMBER 1972

Inelastic Neutron Scattering from Solid Neon*

J. Skalyo, Jr., V. J. Minkiewicz,† and G. Shirane
Brookhaven National Laboratory, Upton, New York 11973

and

W. B. Daniels
University of Delaware, Newark, Delaware 19711

(Received 7 May 1972)

The phonon dispersion curves of a neon sample with a lattice spacing of 4.454 ± 0.002 Å have been measured in the [100], [110], and [111] symmetry directions at 5 °K. Accuracies between 0.5 and 2% are evidenced except for high-energy modes near the zone boundary, i.e., for modes with energies greater than ≈ 6 meV. The data can be fit extremely well with an axially symmetric four-neighbor force-constant model of eight parameters. Measurements made at $\zeta < 0.2$ allowed an accurate determination of the zero-sound elastic constants $C_{11} = 166.1 \pm 1.7$, $C_{12} = 85.5 \pm 2.1$, and $C_{44} = 95.2 \pm 0.5 \times 10^8$ dyn cm^{-2}. The latter give a value for the zero-sound bulk modulus $B_0 = \frac{1}{3}(C_{11} + 2C_{12}) = 112.4 \pm 1.7 \times 10^8$ dyn cm^{-2} which agrees with the adiabatic first-sound bulk modulus. Phonon measurements have also been obtained at 22 °K in the [100] direction with no change in sample density. The isochoric temperature shift varies between 1 and 2% for the longitudinal mode and between -3.5 and 0% for the transverse mode as ζ changes from 0.1 to 0.5, respectively. The measured phonon line shapes have also been compared with the instrumental resolution in order to determine intrinsic phonon lifetimes. In most instances, upper limits to the broadening are obtained. For $\zeta < 0.1$, all branches have widths < 0.07 meV at 5 °K. The phonon widths of the [100] branches are considerably broadened by increasing the temperature from 5 to 22 °K. At 22 °K the [100]T phonon at $\zeta = 0.2$ has an energy of 1.45 meV and a width of ≈ 0.3 meV, whereas at 5 °K only an upper limit for the width of < 0.2 meV can be given for all [100]T phonons. The detailed measurement of phonons near the zone boundary with energies greater than 6 meV was not accomplished due to substantial broadening (>1 meV) of the single-phonon response and its superposition by multiphonon scattering, which is broad in energy and of comparable intensity.

I. INTRODUCTION

The rare-gas elements provide ideal substances for comparison of theory and experiment. Due to their inertness, the solid phase is that of a simple molecular crystal whose behavior is largely controlled by an interatomic pair potential; the various thermodynamic properties are related to particular averages of the energy density of states. The inelastic scattering of neutrons from single crystals is a particularly useful method of studying individual excitations and such measurements could therefore present a critical test for theory. The first such experimental investigation was done at Brookhaven National Laboratory by Daniels *et al.*[1] on a single crystal of krypton.

They showed that a simple quasiharmonic model utilizing a Lennard–Jones (LJ) potential could give agreement with the data. More accurate potentials have also been used by Barker *et al.*[2] to fit the data, indicating a present need for more precise measurements, especially in order to check the nature of the three-body forces. Subsequent advances in measurement technique permitted the